Planta (2010) 232:807–815
DOI 10.1007/s00425-010-1213-y

ORIGINAL ARTICLE

Non-invasive microelectrode potassium flux measurements as a potential tool for early recognition of virus–host compatibility in plants

Sergey Shabala · Olga Babourina · Zed Rengel · Lev G. Nemchinov

Received: 13 January 2010 / Accepted: 20 June 2010 / Published online: 10 July 2010

Abstract Diseases caused by plant viruses are widespread, resulting in severe economic losses worldwide. Understanding the cellular basis of defense responses and developing efficient diagnostic tools for early recognition of host specificity to viral infection is, therefore, of great importance. In this work, non-invasive ion selective microelectrodes (the MIFE technique) were used to measure net ion fluxes in mesophyll tissue of host (potato, tomato, tobacco) and non-host (sugar beet and periwinkle) plants in response to infection with *Potato virus X* (PVX). These results were complemented by FLIM (Fluorescence Lifetime Imaging) measurements of PVX-induced changes in intracellular Ca^{2+} concentrations. Our results demonstrate that, unlike in other plant–pathogen interactions, Ca^{2+} signaling appears to be non-essential in recognition of the early stages of viral infection. Instead, we observed significant changes in K^+ fluxes as early as 10 min after inoculation. Results of pharmacological experiments and membrane potential measurements pointed out that a significant part of these fluxes may be mediated by depolarization-activated outward-rectifying K^+ channels. This may suggest that viral infections trigger a different mechanism of plant defense signaling as compared to signals derived from other microbial pathogens; hence, altered Ca^{2+} fluxes across the plasma membrane may not be a prerequisite for all elicitor-activated defense reactions. Clearly pronounced host specificity in K^+ flux responses suggests that the MIFE technique can be effectively used as a screening tool for the early diagnostics of virus–host compatibility.

Keywords Calcium · Host–pathogen interactions · Ion fluxes · Membrane transport · Potassium · Virus–host compatibility

Abbreviations

HR	Hypersensitive response
MIFE	Microelectrode ion flux estimation system
NO	Nitric oxide
PVX	Potato Virus X
ROS	Reactive oxygen species
TEM	Transmission electron microscope
$[Ca^{2+}]_{cyt}$	Cytosolic free Ca^{2+}
FLIM	Fluorescence lifetime imaging confocal microscopy

Introduction

Diseases caused by plant viruses are of substantial agricultural importance worldwide. Economic losses due to the viral pathogenesis can be huge, especially in major farming

Electronic supplementary material The online version of this article (doi:10.1007/s00425-010-1213-y) contains supplementary material, which is available to authorized users.

S. Shabala (✉)
School of Agricultural Science and Tasmanian Institute of Agricultural Research, University of Tasmania, Private Bag 54, Hobart, Tasmania 7001, Australia
e-mail: Sergey.Shabala@utas.edu.au

O. Babourina · Z. Rengel
School of Earth and Environment, The University of Western Australia, Crawley, WA 6009, Australia

L. G. Nemchinov
Molecular Plant Pathology Laboratory, Plant Sciences Institute, USDA/ARS, Beltsville, MD 20705, USA

crops (Waterworth and Hadidi 1998). Susceptibility or resistance of host plants to viruses depends on a variety of factors, most of which are presumably of genetic nature. It is particularly true and relatively well-studied in the case of inherited resistance to a specific virus, defined as host resistance, whereby spread of the viral pathogen throughout the plant is limited (Kang et al. 2005). In contrast, non-host resistance is characterized by inability of a virus to infect a plant (Heath 2000; Thordal-Christensen 2003; Kang et al. 2005).

Knowing whether plants are susceptible to pathogen may determine a range of measures associated with crop production, such as introduction, management, and potential yield. Even though there is an extensive knowledge on major viruses infecting most important crops, a host range of already known pathogens is constantly expanding, with the Matthew's Plant Virology estimating more than 25×10^6 new compatible host–virus combinations awaiting discovery (Hull 2002).

Although plant virology diagnostic protocols have greatly improved over the last decade, the host-range studies are mainly done by mechanical inoculation of an array of plant species followed by observations of the development of disease symptoms and back-inoculation to a known host (Hull 2002). Such procedures are time consuming and labor extensive. Hence, a suitable alternative would undoubtedly be beneficial; a quick test of potential virus–host compatibility may be a valuable tool both in practical field virology and in the study of molecular host–pathogen interactions.

Ion fluxes across cellular membranes are known to play the key role in triggering and mediating defense mechanisms in plants. Being arguably the earliest measurable responses in plants (Zimmermann et al. 1999), they mediate the activation of signal transduction pathways, alternation of transcriptional profiles, generation of reactive oxygen species (ROS), and production of nitric oxide (NO) and other signal molecules, leading to the induction of defense responses against pathogens (Grant et al. 2000; Lam et al. 2001). In spite of considerable economic importance of plant viruses and therefore the implications of studies related to host defense mechanisms against viral infections, little or no data are currently available on ion signatures generated during plant–virus interactions.

In this work, we used non-invasive ion selective microelectrodes (the MIFE technique) to measure net ion fluxes from mesophyll tissue of host and non-host plants in response to infection with *Potato virus X*, the most widespread of all the potato viruses that infects several *Solanaceous* crops including potato, tomato and tobacco. Our results demonstrate that, unlike in other plant–pathogen interactions, Ca^{2+} signaling appears to be non-essential in recognition of the early stages of viral infection. Instead, we observed significant changes in K^+ fluxes as early as 10 min after inoculation. This may suggest that viral infections trigger ionic currents associated with plant defense signaling that differ from ion fluxes induced by other microbes. In addition, our results indicate that Ca^{2+} fluxes across the plasma membrane may not be a prerequisite for all elicitor-activated defense reactions (cf. Jabs et al. 1997). The clearly pronounced host specificity in K^+ flux responses to viral infection also suggests that using MIFE technique to measure changes in membrane-transport activity in plant tissues can be an effective screening tool for early diagnostics of virus–host compatibility.

Materials and methods

Plant material, inoculation and virus purification

Tobacco (*Nicotiana benthamiana* L.), tomato (*Lycopersicon esculentum* L.), potato (*Solanum tuberosum* L.), periwinkle (*Vinca minor* L.) and sugar beet (*Beta vulgaris* L.) (all from USDA/ARS, Beltsville, MD, USA) were grown in the containment greenhouse facilities either at the Molecular Plant Pathology Laboratory (USDA/ARS, Beltsville, MD, USA) or at the University of Tasmania (Hobart, Australia) glasshouse, with supplemental lamp illumination and a photoperiod of 16 h. For virus purification, fully expanded leaves of *Nicotiana benthamiana* were inoculated with capped RNA transcripts generated from the linearized PVX-based vector pP2C2S (obtained from D. Baulcombe, Sainsbury Laboratory, Norwich, UK) using Ambion's T7 mMessage Machine kit (Ambion, Austin, TX, USA). For a second passage, plants were mechanically inoculated with PVX-infected tissue from primary inoculated plants homogenized in 20 mM phosphate buffer at the ratio of 1:4 (w/v). Virus was purified according to the procedure described by AbouHaidar et al. (1998). Viral concentration was calculated using PVX extinction coefficient (2.97) for the values at 260 nm and was 1.9 mg mL^{-1} of the resultant solution. Purified viral preparations were visualized by TEM (see Supplemental Fig. 1) as follows: carbon-coated grids were incubated for 1 min with sucrose gradient-purified virus to capture virions, rinsed by washing with 0.5 mL sterile H_2O over the grid and stained with a 2% (v/v) aqueous solution of uranyl acetate. The grids were examined under a JEOL 100-CXII electron microscope at magnifications of 80,000–200,000.

Pseudomonas syringae pv *syringae* 61 was obtained from N. Mock and C.J. Baker (Molecular Plant Pathology Laboratory, USDA/ARS, Beltsville, MD, USA). Bacteria were grown overnight in 5 mL of King's B (KB) medium (King et al. 1954). The medium was supplemented with 20 μg mL^{-1} of nalidixic acid at 30°C. Inoculum was

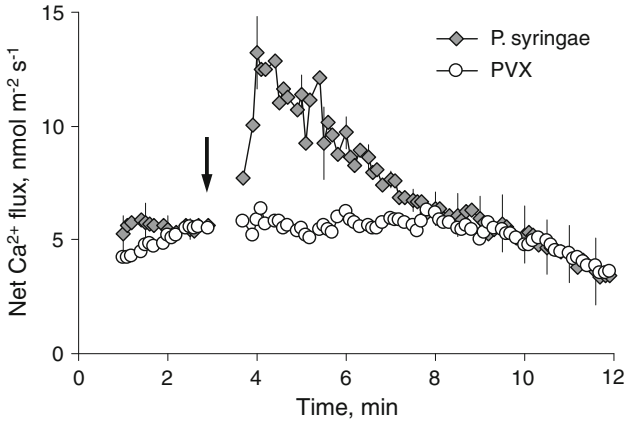

Fig. 1 Transient net Ca^{2+} flux responses from mesophyll segments of *N. benthamiana* in response to the addition of viral (Potato Virus X) and bacterial (*P. syringae*) agent. Mean ± SE ($n = 4$). In all MIFE measurements, the sign convention is "influx positive". *P. syringae* data were adapted from our previous publication (Nemchinov et al. 2008) by normalizing measured Ca^{2+} flux to account for the difference in the background Ca^{2+} concentration to make results comparable in one figure

obtained by harvesting bacteria for 10 min at 2.5*g* in an Eppendorf bench-top centrifuge model 5702 R and suspending in 5 mL of deionized water. After this washing step was repeated twice, the bacterial culture was adjusted to appropriate cell densities of OD_{600} 0.2 (~2×10^8 cells per mL).

Non-invasive Ca^{2+} and K^+ flux measurements

Net fluxes of Ca^{2+}, K^+ and H^+ were measured non-invasively using the microelectrode ion flux measurement (MIFE) technique. All details on microelectrode fabrication and calibration are given in our previous publications (e.g. Shabala and Shabala 2002; Cuin and Shabala 2005), and the full description of the MIFE theory and ion flux calculations procedures are also available elsewhere (Newman 2001; Shabala et al. 2006). The healthy leaves were excised, abaxial epidermis was gently removed as described elsewhere (Shabala and Hariadi 2005) and mesophyll segments of about 3 × 5 mm size were cut and left floating (peeled side down) on a surface of measuring solution [basal salt medium (BSM): 0.1 mM $CaCl_2$ + 0.2 mM KCl; pH 6 unbuffered] for at least 3 h to avoid potential wounding effects.

For treatment, excised mesophyll segments with removed epidermis were placed peeled side down directly on the 50-µL drop of purified viral suspension on Parafilm in a closed 60-mm Petri dish (Supplemental Fig. 2a). Control samples were incubated using measuring solution (see above). The incubation period varied between 10 min and 3 h, depending on the purpose of experiment. After the incubation with PVX, leaf segments were mechanically immobilized in a Perspex holder and placed in a measuring chamber containing ~10 mL of measuring solution (see Supplemental Fig. 2b). The use of the shallow chambers ensured an adequate aeration for the entire duration of experiment (see Zivanovic et al. 2005 and Pang et al. 2006 for more details on oxygen levels in the bath solution).

Ion-selective microelectrodes were positioned 50 µm above the mesophyll surface. During the measurements, electrodes were moved back and forth in a square-wave manner by a computerized stepper motor between two positions (50 and 120 µm above the leaf surface) with 0.125 Hz frequency. Net ion fluxes were calculated from measured differences in the electrochemical potential between these two positions for each ion, as described earlier (Shabala et al. 1997). Measurements were conducted under either dim (20 µmol s^{-1} m^{-2}) or bright light (2,500 µmol s^{-1} m^{-2}) using inverted microscope model RTC-6 (Radical Instruments, India).

The immediate ion flux responses were measured by addition of the purified viral or bacterial preparation directly to the measuring chamber with attached leaf sample as described elsewhere (Nemchinov et al. 2008).

Conventional confocal and fluorescence lifetime imaging (FLIM) measurements

Calcium GreenTM AM (Ca-Green-AM, Molecular probes, Eugene, OR, USA) was dissolved in dimethylsulphoxide (DMSO, Sigma, Castle Hill, Australia) and diluted with a loading solution (0.2 mM $CaCl_2$ and 50 mM mannitol, pH 4.2) to a final concentration of 20 µM. The final concentration of DMSO in the loading solution was 1% v/v. Peeled mesophyll segments were placed for 2 h on top of the loading solution in Petri dishes on ice in dark, which was followed by plant cells recovery in the BSM solution for 30 min at room temperature.

For conventional confocal microscopy and FLIM measurements, mesophyll segments were placed in the chamber on the stage of an inverted confocal microscope (Leica TCS SP2 AOBS, Leica Microsystems, Wetzlar, Germany). Light pulses were generated by a Mai Tai Laser (Spectra Physics, Mountain View, CA, USA) for FLIM microscopy, and by an Argon laser for conventional microscopy. Excitation wavelength was set at 940 nm for FLIM analysis and 488 nm for conventional imaging. Fluorescence was recorded by a photo multiplier between 500 and 692 nm.

The FLIM analysis was performed using SPC-730 electronics and SPC7.22 software (both from Becker and Hickl, Berlin, Germany) for time-correlated single-photon counting (O'Connor and Desmond 1984). Lifetime images were analyzed using SPCImage 2.6 (Becker and Hickl).

For the FLIM calibration of cytosolic Ca^{2+} activity ($[Ca^{2+}]_{cyt}$), a stock solution of Ca-Green potassium salt was prepared in a 0 mM Ca^{2+} buffer (Calcium Calibration

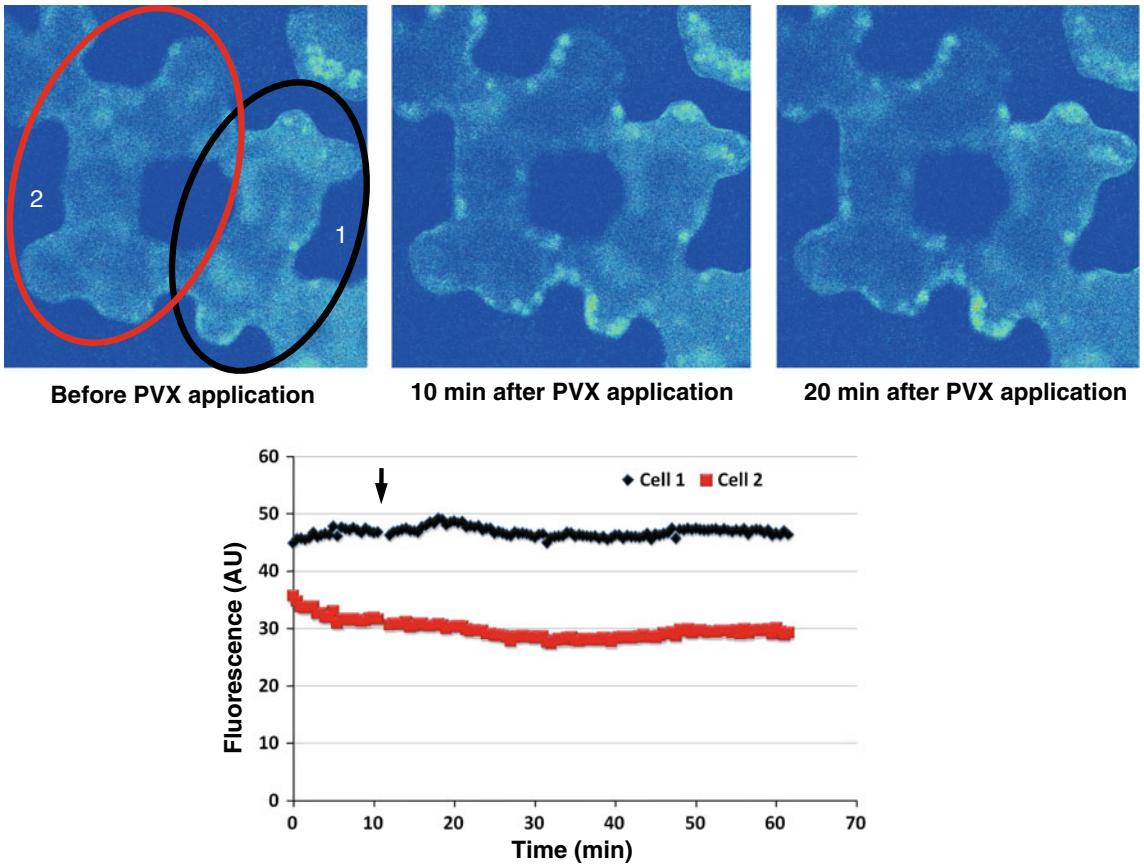

Fig. 2 Changes in Ca-Green fluorescence in mesophyll cells in response to Potato Virus X (PVX) treatment (added at 10 min as indicated by an *arrow* in the *bottom panel*). *Upper panels* show cells used in calculation of the average fluorescence intensity in the region of interest (ROI). A representative experiment is shown (out of five)

Kit #2, Molecular Probes), as described earlier (Guo et al. 2009). For Ca^{2+} concentration calibration, a ratio between intensities of the first (short) and the second (long) components was used.

Pharmacological experiments

Several known ion channel blockers such as TEA^{+} (20 mM), Gd^{3+} (50 μM) and Cs^{+} (100 μM) were used in electrophysiological experiments to specify the nature of transport system mediating the observed K^{+} flux. All the inhibitors were added to leaf samples after 3 h of inoculation with PVX, 20–30 min prior to flux measurements. In additional experiments, some of these blockers were mixed with purified viral preparations prior to mechanical leaf inoculation in the glasshouse, followed by the visual observation of development of PVX symptoms on inoculated leaves.

Membrane potential measurements

Conventional KCl-filled Ag/AgCl microelectrodes (Cuin and Shabala 2005) with tip diameter ~0.5 μm were used. Measurements were taken from at least four individual leaf segments for each treatment. Membrane potentials were typically recorded for 1–1.5 min after initial cell penetration before moving to another spot on the leaf surface.

Statistical analysis

Statistical significance of mean values was determined using the standard Student's *t* test at $P \leq 0.05$ level.

Results

Addition of the purified PVX preparation to the mesophyll tissue of *N. benthamiana* caused no change in the rate of Ca^{2+} transport across the plasma membrane (Fig. 1; open symbols), This is in contrast to the effect of bacteria, whereby addition of *P. syringae* to the mesophyll tissue of *N. benthamiana* caused a rapid, transient net Ca^{2+} influx that peaked at ~1 min after the pathogen application and gradually decreased over the next 5–8 min (Fig. 1; closed symbols). Also, no significant (at $P \leq 0.05$) elevation

change in $[Ca^{2+}]_{cyt}$ was observed for at least 50 min after PVX inoculation (Fig. 2). Moreover, after 3-h exposure of tobacco mesophyll to PVX, there was a small but significant ($P \leq 0.05$) decrease in $[Ca^{2+}]_{cyt}$ (Fig. 3). At the same time, a clearly pronounced transient elevation in $[Ca^{2+}]_{cyt}$ was measured in response to NaCl treatment in tobacco mesophyll cells (Supplemental Fig. 3). This is consistent with previous reports on other plant systems (Knight et al. 1997; Tracy et al. 2008) and validates the use of the confocal microscopy technique. Taken together, our results suggest that Ca^{2+} uptake might not be critical for plant–viral interaction.

The 3-h incubation with purified virus caused a significant ($P < 0.001$) and massive net K^+ efflux (100–150 nmol m^{-2} s^{-1}) from tobacco mesophyll cells (Fig. 4). This viral-induced activation of K^+ efflux systems appeared highly host specific because it was observed only in potato, tomato, and tobacco—known hosts for the virus (Büchen-Osmond 2006), but not in non-host species (sugar beet and periwinkle) (Fig. 5b). At the same time, no significant difference between net Ca^{2+} fluxes was observed between

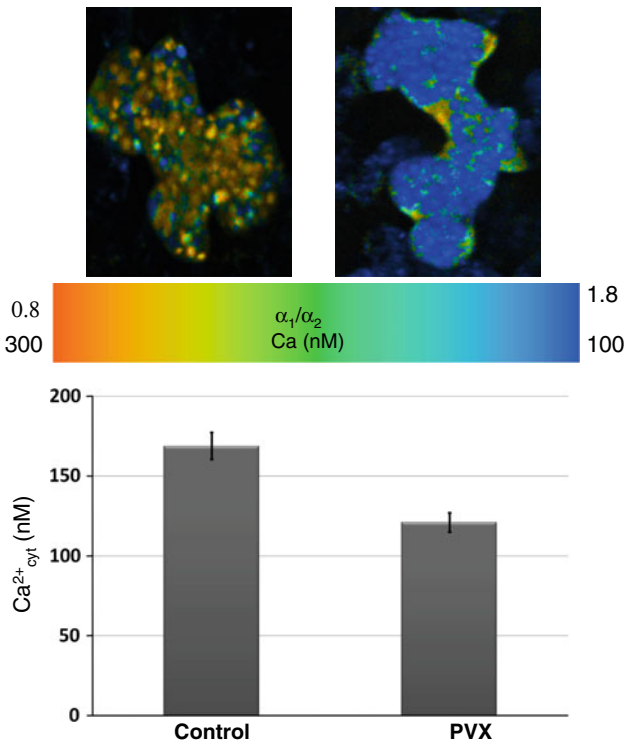

Fig. 3 Changes in the intracellular Ca^{2+} concentration in mesophyll cells exposed to basal salt medium (BSM, control) and PVX for 3 h. *Upper panels* show the pseudo-color FLIM images. The ratio of intensities of the fast and slow component of Ca-Green fluorescence lifetime is shown in colour as $\alpha 1/\alpha 2$ distribution. Lower Ca^{2+} concentrations appear in the *blue* colour, and the higher Ca^{2+} concentration appears in the *yellow* colour. The *bottom graph* shows calculated intracellular Ca^{2+} concentration in control and PVX-treated cells. Mean ± SE (n = 8–13)

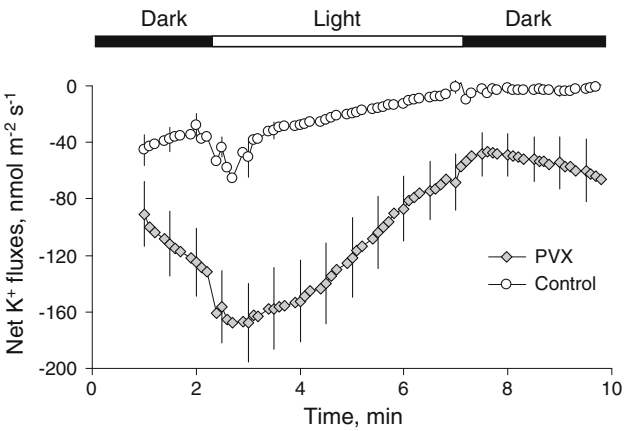

Fig. 4 Light-induced changes in net K^+ fluxes measured from mesophyll surface of *N. benthamiana* plants after 3 h of inoculation with PVX. Mean ± SE (n = 4–6)

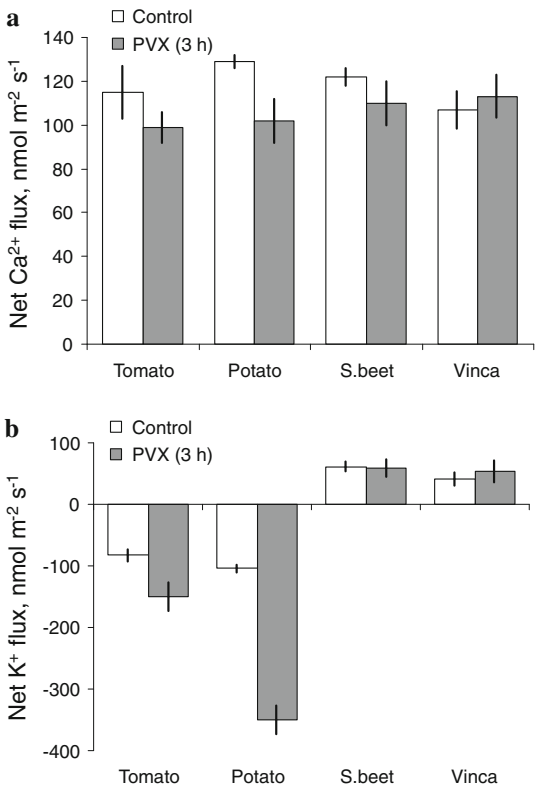

Fig. 5 Steady-state net Ca^{2+} (**a**) and K^+ (**b**) fluxes measured from the light-exposed mesophyll tissues of two host (tomato, potato) and two non-host (beet and periwinkle) species after 3 h of inoculation with PVX. Mean ± SE (n = 4–6)

PVX-treated and control plants for either host- or non-host species after 3 h of treatment (Fig. 5a).

To elucidate ionic mechanisms underlying perception and intracellular signaling of the virus, a series of pharmacological experiments was undertaken. In one of these, some known blockers of K^+-permeable ion channels (e.g. TEA^+ and Gd^{3+}) were mixed with purified viral preparations prior

to mechanical leaf inoculation. The results (Fig. 6a) suggest that addition of either blocker to the leaf alongside with PVX did not ameliorate infections symptoms. However, both TEA^+ and Gd^{3+} were highly effective in preventing PVX-induced K^+ efflux from tobacco mesophyll cells (Fig. 6b); a similar effect was achieved with another known blocker of K^+-permeable non-selective cation channels, Cs^+ (Fig. 6b). Among the three K^+-channel inhibitors, TEA^+ was the most efficient blocker (~90% inhibition), followed by Cs^+ and Gd^{3+} (~70–75% inhibition) (Fig. 6b).

Three hours of incubation with PVX caused significant ($P < 0.001$) membrane depolarization (from -119 ± 1.6 to -85 ± 1.9 mV) in tobacco mesophyll cells (data not shown).

From Fig. 5b data, it appears that the PVX-host species such as tomato and potato showed net efflux of K^+ (open bars in Fig. 5b), while the non-host species sugar beet and periwinkle showed small but significant ($P \leq 0.05$) net K^+ uptake. To ascertain that this difference in the initial fluxes (and hence, susceptibility to viral infection) was not attributed to the sample damage during preparation (epidermis peeling), measurements of the plasma membrane potential were compared between peeled and unpeeled mesophyll cells of one host (tomato) and one non-host (periwinkle) species. Although leaf epidermis was slightly more hyperpolarized compared with mesophyll tissue in both tomato and periwinkle (Table 1), membrane potential of peeled and unpeeled mesophyll cells was not significantly different (at $P \leq 0.05$) in the two species, ruling out a possibility of the different extent of the leaf damage as a basis for differential susceptibility to the virus.

Table 1 Plasma membrane potential of mesophyll and epidermal leaf cell in host (tomato) and non-host (periwinkle) species before and after peeling of leaf epidermis.

Treatment	Tomato	Periwinkle
Peeled	-139 ± 2.9	-114 ± 2.1
Non-peeled	-136 ± 1.8	-121 ± 2.4
Epidermis	-154 ± 3.3	-123 ± 1.9

Mean ± SE ($n = 12$–20)

Further insights into the underlying ionic mechanisms were obtained by studying time dependence of PVX effects on net K^+ fluxes. A significant ($P < 0.001$) increase in K^+ efflux was measured as early as 10 min after PVX exposure, and the magnitude of net K^+ efflux did not change much afterward (Fig. 7a). This time dependence of PVX effects on K^+ flux was mirrored by the subsequent changes in net H^+ fluxes (Fig. 7b), with PVX-treated segments showing smaller net H^+ uptake compared with the control (at $P \leq 0.05$), regardless of the time of exposure (Fig. 7b). Again, statistically significant effects of PVX were observed as early as 10 min after PVX application.

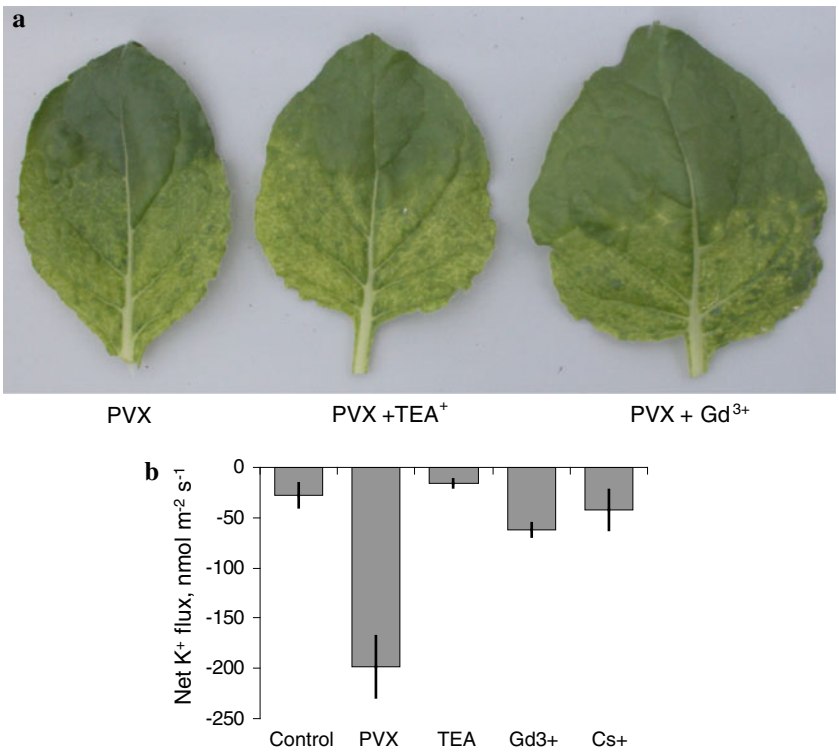

Fig. 6 Pharmacology of PVX inoculation in tobacco leaves. **a** Typical tobacco leaves 10 days after PVX inoculation in the presence or absence of known blockers of K^+-permeable channels, TEA^+ (20 mM) or Gd^{3+} (50 μM). **b** Effect of known blockers of K^+-permeable channels on the magnitude of net K^+ flux from tobacco leaf mesophyll cells after 3 h of inoculation with PVX. Mean ± SE ($n = 4$–6)

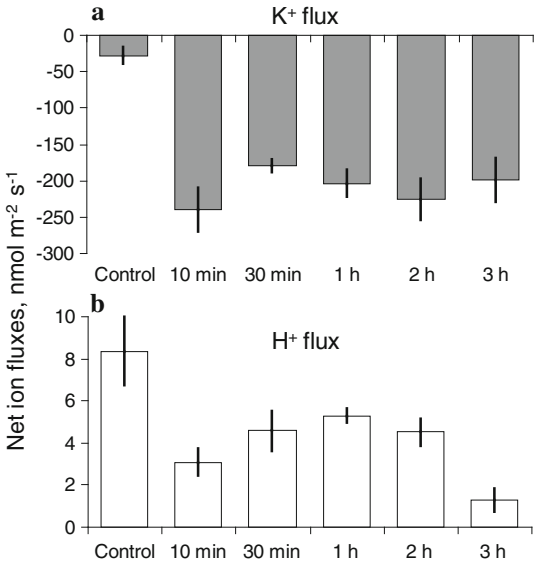

Fig. 7 Time dependence of the effects of PVX inoculation on net K^+ (**a**) and H^+ (**b**) fluxes in tobacco leaves. Mean ± SE ($n = 6$)

Discussion

An important role of ion fluxes in plant defense signaling is well documented. Of these, elicitor-induced transient Ca^{2+} influx from the external environment into the cytosol has always been named as a key element of the signaling cascade and appears to be crucial in the induction of plant defense against pathogens (Scheel 1998; Zimmermann et al. 1999; Blume et al. 2000; Grant et al. 2000). Similar results are reported here for *P. syringae* using the MIFE technique (Fig. 1). Our previous studies have shown that the observed transient Ca^{2+} influx is sensitive to La^{3+} or Gd^{3+} and, hence, is mediated by Ca^{2+}-permeable channels at the plasma membrane of mesophyll cells (Nemchinov et al. 2008).

An addition of the purified PVX preparation to the tobacco mesophyll tissue caused no changes in the rate of Ca^{2+} transport across the plasma membrane (Fig. 1; open symbols). Also, no significant changes in $[Ca^{2+}]_{cyt}$ were detected for at least 50 min after PVX treatment (Fig. 2), suggesting that Ca^{2+} release from internal stores was also not a part of the signal transduction mechanism in plant–viral interaction. Taken together, these results suggest that, contrary to bacterial pathogens, rapid Ca^{2+} signaling may not be essential for the viral perception and initiation of downstream transduction pathway. However, massive K^+ efflux was measured as early as 10 min after PVX inoculation (Fig. 7a), showing all signs of host specificity (Fig. 5b). It should also be commented that the prolonged exposure (3 h) to PVX resulted in lower $[Ca^{2+}]_{cyt}$ levels compared with control plants (Fig. 3). This may be indicative of the role of Ca^{2+} efflux systems in downstream cascades of the plant responses to viral infection, similar to what we observed previously in a case of *P. syringae* pv *syringae* 61 (Nemchinov et al. 2008).

Surprisingly, little is known about the ion fluxes generated during plant–virus interactions, despite significant losses caused by viruses to agricultural crops. So far, we were able to find only few related papers in the literature. Schvarzstein (1997) describes the early events that occur in non-host hypersensitive response (HR) to papaya mosaic virus (PMV) using a patch-clamp technique. It reports that the addition of PMV virus to the patch pipette caused a decrease in the average inward currents and an increase in the outward currents from protoplasts isolated from *Gomphrena globosa* leaf tissue. No change in the plasma membrane average currents was observed when PMV virus was added to the bath solution. It was suggested that several ions such as K^+, Cl^-, gluconate and Ca^{2+} may contribute to the above currents, and that the cell membrane damage is required for viral infection (Schvarzstein 1997).

The phenomenon of rapid K^+ release from host cells during the early phase of viral infection was reported recently (Neupartl et al. 2008). Infection of *Chlorella* cells by *Paramecium bursari* chlorella virus (PBCV-1) produced rapid depolarization of the host by incorporation of viral-encoded K^+ channels (Kcv) into the host membrane. Similar to our data reported here (Fig. 6b), K^+ efflux was partially reduced by blockers of Kcv channels (specifically by Cs^+). Also, the reported kinetics of Kcv incorporation (half-time of cell wall degradation = 2 min; half-time of DNA injection = 4.1 min; Neupartl et al. 2008) is similar to our data showing massive K^+ efflux from host-specific cells as early as 10 min after infection (Fig. 7). Thus, based on the three lines of evidence we reported in the present paper—(a) membrane depolarization, (b) pharmacological evidence, and (c) kinetics of PVX-induced K^+ efflux—one can suggest that the incorporation of a viral K^+-efflux channel into the plasma membrane of host cells may be responsible for the rapid K^+ release from host cells during the early phase of viral infection. Due to the weak specificity of known plant channel blockers (e.g. Zhao et al. 2007), the identity of the channels involved has to be elucidated in direct patch-clamp experiments.

The physiological role of the observed viral-induced K^+ efflux also needs further investigation. It was suggested by Neupartl et al. (2008) that the efflux of K^+ and the associated water efflux from the cell may be needed to reduce turgor and lower the pressure barrier, to aid ejection of DNA from the virus particles into the host. However, adding several known blockers of K^+ efflux channels to the buffer media during PVX inoculation did not ameliorate infection symptoms (Fig. 6a). Several possible explanations can be given. First, the blocking effect of pharmacological agents

was only partial (Fig. 6b), and K^+ efflux from cells could have still been sufficient to facilitate viral DNA ejection into the host. Second, the physiological role of K^+ efflux may not only be related to the cell turgor regulation. With over 50 enzymes being activated by potassium (Marschner 1995; Shabala 2003), potassium homeostasis is central to plant adaptive responses to environment (Amano et al. 1997; Huh et al. 2002; Shabala et al. 2007), including programmed cell death (PCD). Experiments with K^+ ionophores (Inai et al. 1997; Marklund et al. 2001) and apoptotic triggers like dexamethasone (Benson et al. 1996) provided explicit evidence that excessive K^+ efflux and intracellular K^+ depletion are the key early steps in apoptosis (one form of the PCD) in mammalian systems. A critical role for potassium homeostasis in the apoptotic process has been also endorsed for plants (Huh et al. 2002, Shabala et al. 2007; Shabala 2009), yeasts (Huh et al. 2002) and algae (Affenzeller et al. 2009). According to the recent models (reviewed by Shabala 2009), cytosolic K^+ depletion (originating from net K^+ efflux across the plasma membrane) activates caspase-like proteases (Piszczek and Gutman 2007), leading to PCD. Thus, the observed massive net K^+ efflux measured from PVX-inoculated cells (Figs. 4b, 5b) may be considered as an important step in the cell's transition toward PCD.

The observed viral-induced activation of K^+ efflux systems appears to be a highly host-specific process (Fig. 5b). Apparently, this implies that the observed K^+ fluxes are related to the plant's ability to recognize compatible viral infection and activate defence pathways. However, no difference in PVX-induced net Ca^{2+} fluxes was found between the host- and non-host species (Fig. 5a). These results highlight the importance of potassium fluxes in early pathogen recognition events and, specifically, in plant responses to the viral challenge.

As commented above, the exact identity of ion transporters mediating PVX-induced K^+ efflux from leaf mesophyll is clearly beyond the aims of this study. Several virus-encoded K^+-permeable channels were reported in various plant systems (Plugge et al. 2000; Balss et al. 2008), and it remains to be shown if PVX virus operates in a similar mode. As for now, our data demonstrate the importance of potassium homeostasis in plant biotic stress responses and suggest that the measurement of viral-induced K^+ flux from plant tissue may be used as an efficient tool for early recognition of host specificity to viral infection in plants. Given the fact that a clear-cut difference between host- and non-host K^+ flux responses was evident as early as 10 min after leaf inoculation, while the visual symptoms of infection on indicator plants are normally observed only after a week or two, the advantage of the MIFE method for rapid screening for virus–host compatibility is obvious.

Acknowledgments This work was supported by the Australian Research Council and University of Tasmania funding to S.S., ARC funding to Z.R. and by the United States Department of Agriculture, Agricultural Research Service to L.G.N. The microscopy part of this study was carried out using facilities at the Centre for Microscopy, Characterisation and Analysis, The University of Western Australia, which are supported by university, state and federal funding.

References

AbouHaidar MG, Xu KL, Hefferon H (1998) Potexvirus isolation and RNA extraction. Methods Mol Biol 81:131–143

Affenzeller MJ, Dareshouri A, Andosch A, Lutz C, Lutz-Meindl U (2009) Salt stress-induced cell death in the unicellular green alga *Micrasterias deticulata*. J Exp Bot 60:939–954

Amano M, Toyoda K, Ichinose Y, Yamada T, Shiraishi T (1997) Association between ion fluxes and defense responses in pea and cowpea tissues. Plant Cell Physiol 38:698–706

Balss J, Papatheodorou P, Mehmel M, Baumeister D, Hertel B, Delaroque N, Chatelain FC, Minor DL, Van Etten JL, Rassow J, Moroni A, Thiel G (2008) Transmembrane domain length of viral K^+ channels is a signal for mitochondria targeting. Proc Natl Acad Sci USA 105:12313–12318

Benson RSP, Heer S, Dive C, Watson AJM (1996) Characterization of cell volume loss in CEM-C7A cells during dexamethasone-induced apoptosis. Amer J Physiol Cell Physiol 270:C1190–C1203

Blume B, Nürnberger T, Nass N, Scheel D (2000) Receptor-mediated increase in cytoplasmic free calcium required for activation of pathogen defense in parsley. Plant Cell 12:1425–1440

Büchen-Osmond C (2006) Index to ICTVdB virus descriptions. In: ICTVdB—the universal virus database, version 4. Columbia University, NY

Cuin TA, Shabala S (2005) Exogenously supplied compatible solutes rapidly ameliorate NaCl-induced potassium efflux from barley roots. Plant Cell Physiol 46:1924–1933

Grant M, Brown I, Adams S, Knight M, Ainslie A, Mansfield J (2000) The RPM1 plant disease resistance gene facilitates a rapid and sustained increase in cytosolic calcium that is necessary for the oxidative burst and hypersensitive cell death. Plant J 23:441–450

Guo K-M, Babourina O, Rengel Z (2009) Na^+/H^+ antiporter activity of the SOS1 gene: lifetime imaging analysis and electrophysiological studies on Arabidopsis seedlings. Physiol Plant 137:155–165

Heath MC (2000) Nonhost resistance and nonspecific plant defenses. Curr Opin Plant Biol 3:315–319

Huh G-H, Damsz B, Matsumoto TK, Reddy MP, Rus AM, Ibeas JI, Narasimhan ML, Bressan RA, Hasegawa PM (2002) Salt causes ion disequilibrium-induced programmed cell death in yeast and plants. Plant J 29:649–659

Hull R (2002) Matthew's plant virology, 4th edn. Academic Press, San Diego

Inai Y, Yabuki M, Kanno T, Akiyama J, Yasuda T, Utsumi K (1997) Valinomycin induces apoptosis of ascites hepatoma cells (AH-130) in relation to mitochondrial membrane potential. Cell Struct Funct 22:555–563

Jabs T, Tschope M, Colling C, Hahlbrock K, Scheel D (1997) Elicitor-stimulated ion fluxes and O_2^- from the oxidative burst are essential components in triggering defense gene activation and phytoalexin synthesis in parsley. Proc Natl Acad Sci USA 94:4800–4805

Kang B-C, Yeam I, Jahn MM (2005) Genetics of plant virus resistance. Annu Rev Phytopathol 43:581–621

King EO, Ward MK, Raney DE (1954) Two simple media for the demonstration of pyocyanin and fluorescein. J Lab Clin Med 22:301–307

Knight H, Trewavas AJ, Knight MR (1997) Calcium signalling in *Arabidopsis thaliana* responding to drought and salinity. Plant J 12:1067–1078

Lam E, Kato N, Lawton M (2001) Programmed cell death, mitochondria and the plant hypersensitive response. Nature 411:848–853

Marklund L, Henriksson R, Grankvist K (2001) Cisplatin-induced apoptosis of mesothelioma cells is affected by potassium ion flux modulator amphotericin B and bumetanide. Int J Cancer 93:577–583

Marschner H (1995) The mineral nutrition of higher plants. Academic Press, London

Nemchinov LG, Shabala L, Shabala S (2008) Calcium efflux as a component of the hypersensitive response of *Nicotiana benthamiana* to *Pseudomonas syringae*. Plant Cell Physiol 49:40–46

Neupartl M, Meyer C, Woll I, Frohns F, Kang M, Van Etten JL, Kramer D, Hertel B, Moroni A, Thiel G (2008) Chlorella viruses evoke a rapid release of K^+ from host cells during the early phase of infection. Virology 372:340–348

Newman IA (2001) Ion transport in roots: measurements of fluxes using ion-selective microelectrodes to characterize transporter function. Plant Cell Environ 24:1–14

O'Connor DV, Desmond P (1984) Time-correlated single photon counting. Academic Press, London, p 288

Pang JY, Newman I, Mendham N, Zhou M, Shabala S (2006) Microelectrode ion and O_2 fluxes measurements reveal differential sensitivity of barley root tissues to hypoxia. Plant Cell Environ 29:1107–1121

Piszczek E, Gutman W (2007) Caspase-like proteases and their role in programmed cell death in plants. Acta Physiol Plant 29:391–398

Plugge B, Gazzarrini S, Nelson M, Cerana R, Van Etten JL, Derst C, DiFrancesco D, Moroni A, Thiel G (2000) A potassium channel protein encoded by Chlorella virus PBCV-1. Science 287:1641–1644

Scheel D (1998) Resistance response physiology and signal transduction. Curr Opin Plant Biol 1:305–310

Schvarzstein M (1997) Changes in host plasma membrane ion fluxes during the *Gomphrena globosa*–Papaya Mosaic Virus interaction. MSc Thesis, Department of Botany, University of Toronto, Canada

Shabala S (2003) Regulation of potassium transport in leaves: from molecular to tissue level. Ann Bot 92:627–634

Shabala S (2009) Salinity and programmed cell death: unravelling mechanisms for ion specific signalling. J Exp Bot 60:709–711

Shabala S, Hariadi Y (2005) Effects of magnesium availability on the activity of plasma membrane ion transporters and light-induced responses from broad bean leaf mesophyll. Planta 221:56–65

Shabala S, Shabala L (2002) Kinetics of net H^+, Ca^{2+}, K^+, Na^+, NH_4^+, and Cl^- fluxes associated with post-chilling recovery of plasma membrane transporters in *Zea mays* leaf and root tissues. Physiol Plant 114:47–56

Shabala SN, Newman IA, Morris J (1997) Oscillations in H^+ and Ca^{2+} ion fluxes around the elongation region of corn roots and effects of external pH. Plant Physiol 113:111–118

Shabala L, Ross T, McMeekin T, Shabala S (2006) Non-invasive microelectrode ion flux measurements to study adaptive responses of microorganisms to the environment. FEMS Microb Rev 30:472–486

Shabala S, Cuin TA, Prismall L, Nemchinov LG (2007) Expression of animal CED-9 anti-apoptotic gene in tobacco modifies plasma membrane ion fluxes in response to salinity and oxidative stress. Planta 227:189–197

Thordal-Christensen H (2003) Fresh insights into processes of nonhost resistance. Curr Opin Plant Biol 6:351–357

Tracy FE, Gilliham M, Dodd AN, Webb AAR, Tester M (2008) NaCl-induced changes in cytosolic free Ca^{2+} in *Arabidopsis thaliana* are heterogeneous and modified by external ionic composition. Plant Cell Environ 31:1063–1073

Waterworth HE, Hadidi A (1998) Economic losses due to plant viruses. In: Hadidi A, Khetarpal RK, Koganezawa H (eds) Plant virus disease control. APS Press, St. Paul, pp 1–14

Zhao MG, Tian QY, Zhang WH (2007) Ethylene activates a plasma membrane Ca^{2+}-permeable channel in tobacco suspension cells. New Phytol 174:507–515

Zimmermann S, Ehrhardt T, Plesch G, Muller-Rober B (1999) Ion channels in plant signaling. Cell Mol Life Sci 55:183–203

Zivanovic BD, Pang J, Shabala S (2005) Light-induced transient ion flux responses from maize leaves and their association with leaf growth and photosynthesis. Plant Cell Environ 28:340–352